A Molecular Orbital Study of Model Cytochrome P450 Oxidation of CCl_4 and $CHCl_3$

Andrew T. Pudzianowski,[‡] Gilda H. Loew,*[†] Bruce A. Mico,[§] Richard V. Branchflower,[§] and Lance R. Pohl[§]

Contribution from the Life Sciences Division, SRI International, Menlo Park, California 94025, and Laboratory of Chemical Pharmacology, National Heart, Lung, and Blood Institute, National Institutes of Health, Bethesda, Maryland 20205. *Received May 21, 1982*

Abstract: Aerobic liver microsomal metabolism of CCl_4 generates electrophilic chlorine, while metabolism of $CHCl_3$ and $CDCl_3$ under the same conditions does not. These and other observations on cytochrome P450 mediated aerobic metabolism of halomethanes may be reasonably explained on the basis of reaction mechanisms derived from the examination of reaction paths on halomethane–$O(^3P)$ enthalpy surfaces calculated by the MNDO SCF-MO method. A halosylation mechanism is proposed for oxidative metabolism of CCl_4, in which an initial transformation to trichloromethyl hypochlorite occurs. With loss of its electrophilic chlorine, the hypochlorite can decompose to give phosgene, an observed product in vitro. The metabolism of $CHCl_3$ occurs preferentially via hydroxylation to trichloromethanol, which decomposes to yield phosgene but does not give electrophilic chlorine.

Introduction

Halomethane metabolism is a subject of considerable interest primarily because of the hepatotoxicity associated with this class of compounds.[1-8] Carbon tetrachloride and chloroform are two of the most commonly encountered hepatotoxic halomethanes. The cytochrome P450 dependent aerobic metabolism of such compounds has been extensively investigated recently, and the following important observations have been made.

(a) Phosgene, Cl_2CO, is formed during cytochrome P450 mediated metabolism of $CHCl_3$ and CCl_4;[2-5] in each case the carbonyl oxygen is derived from atmospheric O_2.[3,5]

(b) Metabolism of CCl_4 to Cl_2CO apparently does not involve $CHCl_3$ as an intermediate.[4]

(c) The CCl_3 radical can be trapped when CCl_4 is metabolized by rat liver microsomes aerobically.[7]

(d) The tetrahalomethanes CCl_4, $CBrCl_3$, and CBr_4 all yield electrophilic halogens during aerobic metabolism by rat liver microsomes.[8]

(e) The electrophilic chlorine formed from CCl_4 during aerobic metabolism by liver microsomes is derived exclusively from CCl_4 and not chloride ion.[9]

(f) $CHCl_3$ does not yield electrophilic chlorine during liver microsomal metabolism.[8]

In the present study, we have utilized the formalisms of molecular orbital theory and statistical thermodynamics to suggest explanations for these and other findings. The triplet oxene model, which has been applied to the mechanism of cytochrome P450 mediated hydrocarbon oxidations[10,11] and to hydrogen kinetic isotope effects for methyl group hydroxylations,[12] suggests that carbon–halogen bonds, like C–H bonds, are susceptible to cleavage by triplet oxene. In the case of $CHCl_3$, preferential oxidation of the C–H bond may explain why electrophilic chlorine is not detected during the microsomal metabolism of this compound.

Theoretical Methods

The overall theoretical approach is described in detail elsewhere,[13] and specific applications to the oxene model for cytochrome P450 mechanistic studies have also been discussed elsewhere.[10-12] The MNDO molecular orbital method[14] is employed with its original parameterization for third-row elements,[15] and open-shell calculations use the unrestricted (UHF-based) formalism.[16] Mechanisms for the initial reaction of triplet oxene with a halomethane are derived from searches of the MNDO/UHF $O(^3P)$–halomethane enthalpy surface: using total geometry optimization,[13] reactant and product channels are located along with the lowest saddle point (transition state) connecting them on the surface. Each such reaction path defines an elementary step in a mechanism, and competing paths involving the same molecular system may be compared.[11]

The FORTRAN programs MNDO, NDTS, and NDFOR[17] are used, respectively, to locate enthalpy minima and saddle points and to calculate force constants, normal vibrational modes, and principal moments of inertia for all molecular species and transition states found. Using the standard formulas of statistical thermodynamics,[13,18] total partition functions and entropies at 298 K are obtained for each species. Since the MNDO method is parametrized to reproduce heats of formation at 298 K,[14] thermochemical quantities may be calculated both for equilibrium and activation.

Estimates of kinetic parameters may be made from the Eyring equation in the form

$$k(T) = \frac{kT}{h} \exp(\Delta S^{\ddagger}/R) \exp(-\Delta H^{\ddagger}/RT) \qquad (1)$$

where $k(T)$ is the rate constant, k and h are the Boltzmann and Planck constants, T is the absolute temperature, R is the ideal gas constant, and $\Delta H^{\ddagger}$ and $\Delta S^{\ddagger}$ are respectively the enthalpy and entropy of activation. It was found previously[11] that MNDO

[†] SRI International.
[‡] Present address: The Squibb Institute for Medical Research, P.O. Box 191, New Brunswick, NJ 08903.
[§] National Institutes of Health.

(1) S. D. Kutob and G. L. Plaa, *Toxicol. Appl. Pharmacol.*, **4**, 354 (1962).
(2) D. Mansuy, P. Beaune, T. Cresteil, M. Lange, and J. P. Leroux, *Biochem. Biophys. Res. Commun.*, **79**, 513 (1977).
(3) L. R. Pohl, B. Bhooshan, N. F. Whittaker, and G. Krishna, *Biochem. Biophys. Res. Commun.*, **79**, 684 (1977).
(4) H. Shah, S. P. Hartman, and S. Weinhouse, *Cancer Res.*, **39**, 3942 (1979).
(5) V. L. Kubic and M. W. Anders, *Life Sci.*, **26**, 2151 (1980).
(6) C. R. Wolf, W. G. Harrelson, W. M. Nastainczyk, R. M. Philpot, B. Kalyanaram, and R. P. Mason, *Mol. Pharmacol.* **18**, 553 (1980).
(7) J. L. Poyer, P. B. McCay, E. K. Lai, E. G. Janzen, and E. R. Davis, *Biochem. Biophys. Res. Commun.*, **94**, 1154 (1980).
(8) B. A. Mico, R. V. Branchflower, L. R. Pohl, A. T. Pudzianowski, and G. H. Loew, *Life Sci.*, **30**, 131 (1982).
(9) B. A. Mico and L. R. Pohl, *Fed. Proc., Fed. Am. Soc. Exp. Biol.* **41**, 1222 (1982).
(10) A. T. Pudzianowski and G. H. Loew, *J. Am. Chem. Soc.*, **102**, 5443 (1980).
(11) A. T. Pudzianowski and G. H. Loew, *J. Mol. Catal.*, **17**, 1 (1982).
(12) A. T. Pudzianowski and G. H. Loew, *J. Phys. Chem.*, **87**, 1081 (1983).
(13) M. C. Flanigan, A. Komornicki, and J. W. McIver, Jr., *Mod. Theor. Chem.*, **8**, 1 (1977).
(14) M. J. S. Dewar and W. Thiel, *J. Am. Chem. Soc.*, **99**, 4899 (1977).
(15) M. J. S. Dewar, M. L. McKee, and H. S. Rzepa, *J. Am. Chem. Soc.*, **100**, 3607 (1978).
(16) J. A. Pople and D. L. Beveridge, "Approximate Molecular Orbital Theory", McGraw-Hill, New York, 1970, p 52.
(17) W. Thiel, G. P. Ford, M. McKee, D. Nelson, S. Olivella, H. S. Rzepa, and M. J. S. Dewar. The programs were originally obtained from the N. R.C.C. at Lawrence Berkeley Laboratory and modified in our laboratory.
(18) N. Davidson, "Statistical Mechanics", McGraw-Hill, New York, 1962.

0002-7863/83/1505-3434$01.50/0

Table I. Thermochemical Quantities[a] for All Species Involved in $O(^3P) + CCl_4$ and $O(^3P) + CHCl_3$ Abstraction Reactions

	$O(^3P)$	CCl_4[b]	CCl_4O[c] TS	CCl_3[c]	OCl[c]	$CHCl_3$[b]	Cl_3CHO[e] TS	OH[d]	Cl_2HCClO[e] TS	HCl_2C[e]
ΔH_f°, kcal/mol		−25.4	57.3	−2.1	34.8	−29.1	59.6	0.2	56.8	2.0
	(59.6)	(−22.9)		(18.5)	(24.2)	(−24.6)		(9.4)		(24.1)
S°, cal/(mol K)		74.0	91.1	73.6	54.2	70.5	81.3	43.8	85.2	65.8
	(38.5)	(74.2)		(70.8)	(54.1)	(70.7)		(43.9)		

[a] Experimental values, when available, are given in parentheses in the tables and are derived from Benson's tabulations[21] unless otherwise specified. TS = transition state. [b] Figure 1. [c] Figure 2. [d] Figure 3. [e] Figure 4.

Table II

A. Reaction Thermodynamics at 298 K

reaction	ΔH_r, kcal/mol	ΔS_r, cal/(mol K)	ΔG_r, kcal/mol
$CCl_4 + O(^3P) \rightarrow CCl_3 + OCl$ (3a)	−1.5	15.3	−6.1
	(6.0)	(12.2)	(2.4)
$Cl_3CH + O(^3P) \rightarrow CCl_3 + OH$ (4a)	−32.4	8.4	−34.9
	(−7.1)	(5.5)	(−8.7)
$Cl_2HCCl + O(^3P) \rightarrow Cl_2HC + OCl$ (5a)	6.3	11.0	3.0
	(13.3)		

B. Activation Parameters and Relative Rates at 298 K

reactn	$\Delta H^\ddagger$, kcal/mol	$\Delta S^\ddagger$, cal/(mol K)	$\Delta G^\ddagger$, kcal/mol	rel rate	$\Delta H^\ddagger_{adj}$, kcal/mol	$\Delta G^\ddagger_{adj}$, kcal/mol	rel rate
3a	23.1	−21.4	29.5		5.9	12.3	
4a	29.1 (28.5)[a]	−27.7	37.4	1.0	2.6	10.9	1.0
5a	26.3 (83.6)	−23.8	33.4	860	6.8	13.9	6.3×10^{-3}

[a] The values in parentheses (Table IIB) are for $\Delta E^\ddagger$ obtained from ab initio STO-3G/UHF calculations.

overestimated $\Delta H^\ddagger$ for triplet oxene reactions with hydrocarbons, while giving reliable values for $\Delta S^\ddagger$. Hence, eq 1 yields an approximate value for $\Delta H^\ddagger$ in those cases where a gas-phase rate constant has been measured at 298 K and MNDO has been used to calculate $\Delta S^\ddagger$. Otherwise, the procedure discussed previously[11] must be employed to correct MNDO $\Delta H^\ddagger$ values. The $\Delta H^\ddagger$ values obtained in either manner may then be used to estimate individual rate constants at 298.15 K from the following form of the Eyring equation, in which fundamental constants have been given their numerical values:

$$k = 1.5199 \times 10^{17}\ \text{cm}^3/(\text{mol-s})\ \exp(-\Delta G^\ddagger/0.5925\ \text{kcal/mol}) \quad (2)$$

where $\Delta G^\ddagger$ is the Gibbs free energy of activation. Relative rates for any set of elementary reactions may then be estimated from the corresponding rate constant ratios.

Note that the approach outlined above implies a gas-phase description. The appropriateness of a gas-phase model for reactions occurring in a hydrophobic catalytic site has been discussed previously.[10,11] Thus, it is also possible to draw on experimentally derived gas-phase thermochemical data pertinent to the reactions under consideration, and this has become an integral part of the approach established in previous work[11] on the oxene model.

Results

The reactions studied explicitly with the aid of MNDO involve CCl_4 and $CHCl_3$ as parent halomethanes and Cl_2CO as the common metabolic product. The optimized structures of all three compounds are shown in Figure 1, while their calculated heats of formation at 298 K are given in the tables below and will be referred to separately.

We consider the CCl_4 results first. With $O(^3P)$ we find that direct chlorine abstraction is a viable reaction path, which could then be followed by a recombination and chlorosylation as indicated in eq 3. Optimized structures of the transition state and

Cl abstraction (slow)

$$Cl_3C{-}Cl + O(^3P) \rightarrow Cl_3C + OCl \quad (3a)$$

recombination (chlorosylation)

$$Cl_3C + OCl \rightarrow Cl_3C{-}OCl \quad (3b)$$

the radical products in the abstraction step (3a) are shown in Figure 2, while their calculated heats of formation and entropies are given in Table I. The optimized transition-state structure and the nuclear displacements in the transition mode, or reaction coordinate, shown in Figure 2 clearly indicate the association of the oxygen with Cl_1 and the concomitant flattening of the trichloromethyl group which will lead to the radical products. Note that the transition state is strongly bent with respect to the bonds being broken and formed, in contrast to the collinear hydrogen abstractions found previously[10,11] and the $CHCl_3$ hydrogen abstraction (Figure 4). The off-bond approach of the oxygen in the chlorine abstraction results from overlap requirements involving the oxygen and chlorine orbitals, as well as the availability of the chlorine lone-pair electron density for attack by the oxene radical.

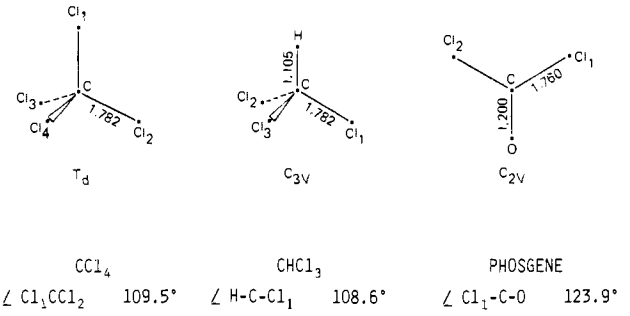

Figure 1. Optimized structures of CCl_4, $CHCl_3$, and $COCl_2$. (All internuclear distances in angstroms.)

The calculated thermochemical and activation parameters for reaction 3a are given in Table II. The CCl_4 abstraction is calculated to be slightly exothermic (Table IIA), while it is actually slightly endothermic. The MNDO/UHF procedure has a nearly systematic tendency to underestimate heats of formation for radicals;[11] hence, the ~10 kcal/mol overestimation of ΔH_f for the OCl radical (Table I) is atypical. Using the most recent[19] rate constant for the gas-phase reaction of $O(^3P)$ with CCl_4 at 300 K together with the MNDO $\Delta S^\ddagger$ value for reaction 3a, the corrected value of $\Delta H^\ddagger$ is found to be 5.9 kcal/mol (Table IIB). Thus, MNDO/UHF overestimates $\Delta H^\ddagger$ by a factor of about 3.9, which is larger than the overestimation found previously for hydrogen abstraction[11] from CH_4.

(19) F. W. Froben, *Ber. Bunsenges. Phys. Chem.*, **72**, 996 (1968).

Table III. Thermochemical Quantities for Proposed Recombination Products and Other Intermediates at 298 K

	Cl_3C-OCl[b]	Cl_3C-OH[c]	Cl_2HC-OCl[c]	OH^- [b]	Cl_3C-O^- [b]	$HOCl$[b]
ΔH_f°, kcal/mol	−19.9	−73.0	−22.0	−5.8 (−33.8)[a]	−131.4	−15.7 (−17.8)
S°, cal/(mol K)	85.0	77.6	79.4	41.0	74.7	56.2 (56.5)

[a] Determined from the proton affinity of OH^- or, alternatively, from the electron affinity of OH radical.[22] [b] Figure 3. [c] Figure 6.

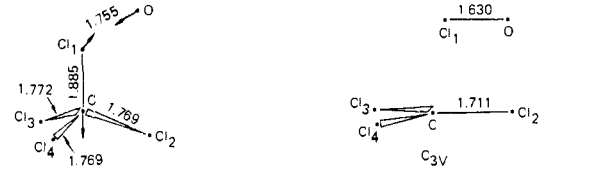

TRANSITION STATE

∠ O-Cl_1-C	141.04°
∠ Cl_1-C-Cl_2	108.72
∠ Cl_1-C-Cl_3	105.61

CCl_3 + OCl

∠ Cl_2-C-Cl_3	119.98°
∠ Cl_2C-CCl_4	119.00

Figure 2. CCl_4 + $O(^3P)$ transition state and products. Note: in this and successive transition states, arrows pointing toward bonds indicate optimized bond lengths, while arrows originating at nuclei show the transition vibrational mode or reaction coordinate.

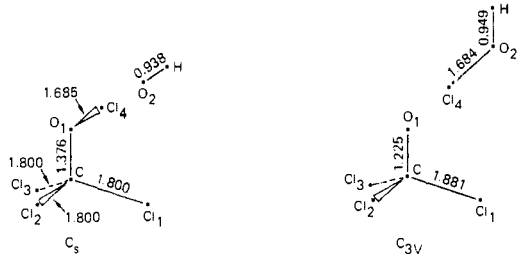

TRICHLOROMETHYL HYPOCHLORITE + HYDROXIDE ION

∠ Cl_4-O_1-C	118.7°
∠ O_1-C-Cl_1	113.1

TRICHLOROMETHOXIDE ION + HYPOCHLOROUS ACID

∠ O_1-C-Cl_1	115.4°
∠ H-O_2-Cl_4	106.4

Figure 3. Cl_3C-OCl + OH^-: reactants and products.

The recombination step (3b) is plausible because the calculated unpaired spin density in the chlorosyl radical (OCl) resides almost exclusively on the oxygen (0.95α spin), thus establishing the analogy between chlorosylation and hydroxylation. The calculated ΔH_f and S° for trichloromethyl hypochlorite are given in Table III, while the optimized structure is shown in Figure 3. We note that the calculated partial charge on the chlorosyl chlorine in trichloromethyl hypochlorite is positive (~0.1), while the oxygen and remaining chlorines carry partial negative charges: O (0.17−), each Cl (0.1−). This strongly suggests that the chlorosyl chlorine here is electrophilic, as in known hypochlorite compounds. In the case of $CHCl_3$ we must consider two possible reaction mechanisms, hydroxylation (4) and chlorosylation (5), as indicated.

H abstraction (slow)

$$Cl_3C\text{-}H + O(^3P) \rightarrow Cl_3C + OH \quad (4a)$$

recombination (hydroxylation)

$$Cl_3C + OH \rightarrow Cl_3C\text{-}OH \quad (4b)$$

Cl abstraction (slow)

$$HCl_2C\text{-}Cl + O(^3P) \rightarrow HCl_2C + OCl \quad (5a)$$

recombination (chlorosylation)

$$HCl_2C + OCl \rightarrow HCl_2C\text{-}OCl \quad (5b)$$

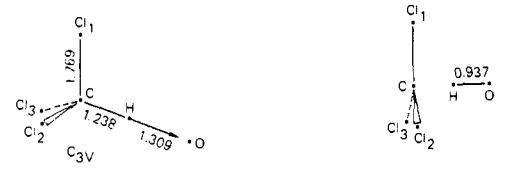

TRANSITION STATE

∠ H-C-Cl_1 106.8°

CCl_3 + OH

Figure 4. $CHCl_3$ + $O(^3P)$ hydrogen abstraction: transition state and products.

TRANSITION STATE

∠ O-Cl_1-C	141.8°
∠ Cl_1-C-H	105.0
∠ Cl_1-C-Cl_2	104.8
∠ Cl_1-C-Cl_3	109.0

DICHLOROMETHYL RADICAL + OCl

∠ H-C-Cl_2 120.1°

Figure 5. $CHCl_3$ + $O(^3P)$ chlorine abstraction: transition state and products.

The transition states and products for the abstraction reactions (4a) and (5a) are shown in Figures 4 and 5, respectively. The transition mode for (4a) shows this reaction to be a pure hydrogen abstraction with a "linear" transition state, as in $O(^3P)$ hydrogen abstractions treated previously.[11] The transition mode (Figure 5) for the $CHCl_3$ chlorine abstraction (5a) closely resembles that for the CCl_4 chlorine abstraction (3a) shown in Figure 2.

Calculated thermochemical quantities for the individual species in both $CHCl_3$ abstractions are given in Table I, and these values lead to the reaction and activation parameters reported in Table II. It will be noted that the calculated entropies in Table I are in excellent agreement with experimentally derived entropies, thus suggesting that the optimized structures of the individual species are reliable.[11]

When the calculated and experimental results for reactions 4a and 5a are compared (Table II), a deficiency of MNDO noted previously[11] is once again apparent. That is, both barriers to reaction, $\Delta H^\ddagger$, are overestimated by MNDO; however, the errors involved in describing a C–H–O transition state are evidently smaller than those for a C–Cl–O transition state. In fact, the errors reverse the expected relative barrier heights for reactions 4a and 5a: (4a) is exothermic according to both the MNDO/UHF results and experimental data, while (5a) is definitely endothermic. Since both reactions occur on the same surface and are similar (abstractions), we fully expect the exothermic (4a) to be faster; but the MNDO results indicate the opposite (Table IIB).

The contention that the MNDO/UHF $\Delta H^\ddagger$ values for reactions 4a and 5a are qualitatively in error is further supported by single point ab initio calculations, at the STO-3G/UHF level of theory, on the reactants and transition states fixed at their MNDO optimized geometries. The resulting $\Delta E^\ddagger$ values are given in Table IIB, and the $\Delta E^\ddagger$ for the chlorine abstraction (5a) is some 55 kcal/mol higher than for the hydrogen abstraction (4a). Along

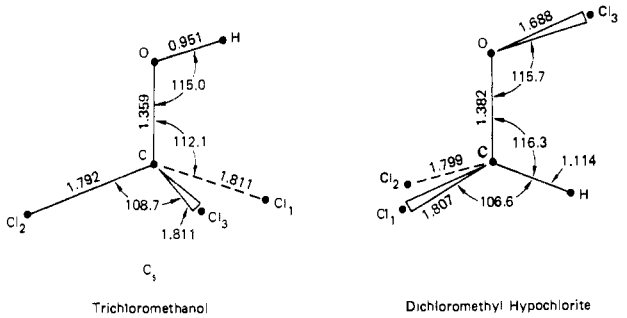

Figure 6. Optimized structures of trichloromethanol and dichloromethyl hypochlorite.

with the individual $\Delta E^{\ddagger}$ values, this difference would be expected to decrease with larger basis sets and more refined treatments of electron correlation, but it is doubtful that the qualitative outcome would be reversed.

From the most recent[19] gas-phase rate constant for $O(^3P)$ + $CHCl_3$ and the MNDO $\Delta S^{\ddagger}$ for hydrogen abstraction, we obtain an estimated $\Delta H^{\ddagger}$ = 2.6 kcal/mol for reaction 4a (Table IIB). For the chlorine abstraction (5a) we assume that the overestimation of $\Delta H^{\ddagger}$ is similar to that for the CCl_4 abstraction (~3.9×), thus arriving at the value of 6.8 kcal/mol given in Table IIB. On the basis of these figures, the hydrogen abstraction (4a) is estimated to be ~160 times faster than the chlorine abstraction (5a) at 298 K.

The recombination products of (4b) and (5b), trichloromethanol and dichloromethyl hypochlorite, respectively, are shown in Figure 6, while their calculated heats of formation and entropies are given in Table III. Like the trichloromethyl hypochlorite product of reaction 3b, these intermediates would most likely form in the hydrophobic catalytic pocket of cytochrome P450, where they would be relatively stable toward decomposition. In a solution environment, however, they would be expected to rapidly undergo solvolysis or some other form of nucleophilic attack directed at the chlorosyl chlorine of the hypochlorites or the hydroxyl hydrogen of trichloromethanol.

The effect of bulk solvent on reactions in solution cannot in general be addressed by gas-phase molecular orbital calculations. However, the electrophilic nature of the chlorosyl chlorine in Cl_3C–OCl, a compound which has not yet been characterized experimentally, can be demonstrated by calculating a reaction path with hydroxide ion as the nucleophile, as shown in eq 6, where

$$Cl_3C\text{–}OCl + OH^- \rightarrow Cl_3C\text{–}O^- + HOCl \qquad (6)$$

the products are trichloromethoxide ion and hypochlorous acid. The optimized structures of the reactants and products are given in Figure 3, while their calculated heats of formation and entropies are reported in Table III. An enthalpy reaction profile for reaction 6 was obtained by fixing the O–Cl distance at a series of increasing values and then allowing all remaining internal coordinates to optimize so as to determine the minimum ΔH_f at each value of the O–Cl "reaction coordinate". The enthalpy profile obtained is typical for a highly exothermic gas-phase ion–molecule reaction, in that there is no barrier and the minimum corresponds to a complex in which the two products are associated. The significant qualitative observation is, of course, that the electrophilic chlorosyl chlorine of trichloromethyl hypochlorite is transferred to the hydroxide ion, yielding the electrophilic chlorinating agent HOCl and a trichloromethoxide ion.

Discussion

The "gas-phase" mechanisms represented by reactions 3 and 4 are consistent with the major experimental observations given in the Introduction. They show how oxygen may be incorporated into CCl_4 and $CHCl_3$ by the same general mechanism already proposed for hydrocarbon oxidation by cytochrome P450.[10,11] Furthermore, they predict the formation of trichloromethyl radicals from both substrates, and they account in a natural way for the formation of electrophilic chlorine, via halosylation of CCl_4. A further prediction is implicit in the preference for hydroxylation over halosylation in $CHCl_3$ oxidation, namely, that electrophilic chlorine is not expected as a product of P450-mediated oxidative metabolism of chloroform. Indeed, electrophilic chlorine has not been observed during the metabolism of either $CHCl_3$ or $CDCl_3$,[20] even though the hydroxylation step is expected to be some 15 times slower in $CDCl_3$ than in $CHCl_3$.[12]

The formation of phosgene is easily accounted for on the basis of the expected solution behavior of the products of reactions 3 and 4. The results already presented suggest that the chlorosyl chlorine of Cl_3C–OCl is electrophilic and susceptible to attack by a nucleophile, and it is clear that elimination of a chloride ion from the resulting trichloromethoxide would also yield phosgene. What is not clear is whether the generation of phosgene from Cl_3C–OCl occurs stepwise, as suggested above, or in a concerted fashion. For the present, the proposed transformation is best written as the overall reaction (7), where :B is simply a general

$$Cl_3C\text{–}OCl + :B \rightarrow Cl_2C{=}O + B{:}Cl^+ + Cl^- \qquad (7)$$

base.

With Cl_3C–OH as an intermediate in chloroform oxidation, the formation of phosgene is accounted for in analogous fashion, this time through elimination of the elements of HCl:

$$Cl_3C\text{–}OH + :B \rightarrow Cl_2C{=}O + B{:}H^+ + Cl^- \qquad (8)$$

Here, we are again not interested in whether the elimination is stepwise (E1) or concerted (E2). Note that only inorganic chloride is expected in reaction 8, while reaction 7 may result in the formation of various halogenated products depending on the nature of the base. For example, if water is the base, a chlorinating agent, hypochlorous acid, is produced. Similarly, reaction with 2,6-dimethylphenol, a typical reagent used to detect electrophilic halogen species,[8] would yield 4-chloro-2,6-dimethylphenol.

The halosylation mechanism presumably applies to CBr_4 and $CBrCl_3$, and both compounds are known to undergo microsomal oxidation and yield electrophilic halogen.[8] The available thermochemical data[21,22] show that reaction 3a is highly endothermic with CF_4 (ΔH_r = 78 kcal/mol at 298 K). Thus, the present mechanism implies that CF_4 should be unreactive toward oxidative P450 metabolism.

On the basis of available gas-phase thermochemical data,[21,22] it is possible to conclude that, for the remaining chloromethanes, CH_2Cl_2 and CH_3Cl, hydrogen abstraction by oxygen is favored over chlorine abstraction and that both C–H and C–Cl bonds weaken with increasing chlorination over the whole chloromethane series. The resulting chloromethanols would be expected to undergo eliminations analogous to reaction 8; hence, the expected products of CH_2Cl_2 and CH_3Cl metabolism would be, respectively, formyl chloride (HClC=O) and formaldehyde (H_2C=O). The same conclusions have been reached previously[23] on the basis of direct mechanistic studies of microsomal oxidations.

Other mechanisms have been proposed for the cytochrome P450 mediated metabolism of tetrahalomethanes to give electrophilic halogens and carbonyl halides.[8] These mechanisms involve reductive pathways and direct interaction of intermediates with superoxide anion radical. The present study, however, indicates for the first time that a halosylation pathway, formally analogous to hydroxylation, is theoretically possible for this class of compounds and provides qualitative mechanistic details that would be difficult to infer from available experimental data alone. Furthermore, the halosylation pathway is fully consistent with the oxene mechanisms already postulated[10-12] for hydrocarbons, which have led to reasonable explanations of secondary kinetic

(20) B. A. Mico, R. V. Branchflower, and L. R. Pohl, unpublished results.
(21) S. W. Benson, "Thermochemical Kinetics", 2nd ed., Wiley-Interscience, New York, 1976.
(22) R. C. Weast, Ed., "Handbook of Chemistry and Physics", 57th ed., CRC Press, Cleveland, 1976, pp F231–F240.
(23) V. L. Kubic and M. W. Anders, *Biochem. Pharmacol.*, **27**, 2349 (1978).

isotope effects and suicide inactivation in P450-mediated epoxidations[11] and primary kinetic isotope effects in methyl group hydroxylations.[12]

It is important to note that the simple oxene model's apparently wide applicability suggests only that the active oxygen species of cytochrome P450 oxidations has radical character. It should not be construed as implying that the enzymatic oxygen is a free atomic oxygen. What has been claimed is that, thus far, the *reactions* of triplet oxene with various organic compounds seem to have a great deal in common with P450-mediated oxidations of the same or similar compounds and have provided a qualitative framework within which a consistent set of mechanisms has been built up. The actual relationship of this oxygen with both the heme iron and the substrate during oxidation remains to be elucidated.

Acknowledgment. Computations were performed on the CDC 7600 computer at Lawrence Berkeley Laboratory and the Computer Resources VAX 11/780 at SRI International. We thank Dr. Dale Spangler for helpful comments and advice and Dr. Tetsuro Oie for performing the ab initio calculations. Support from NIH Grant No. GM 27943-02 and NCI Contract No N01-CP-15730 is gratefully acknowledged. B.A.M. is a Pharmacology Research Associate, National Institute of General Medical Sciences.

Registry No. CCl_4, 56-23-5; $CHCl_3$, 67-66-3; cytochrome P450, 9035-51-2.

Ab Initio Studies of Molecular Geometries. 27. Optimized Molecular Structures and Conformational Analysis of N^{α}-Acetyl-*N*-methylalaninamide and Comparison with Peptide Crystal Data and Empirical Calculations

J. N. Scarsdale,[†] C. Van Alsenoy,[†] V. J. Klimkowski,[†] Lothar Schäfer,*[†] and Frank A. Momany[‡]

Contribution from the Departments of Chemistry, University of Arkansas, Fayetteville, Arkansas 72701, and Memphis State University, Memphis, Tennessee 38152.
Received April 6, 1982

Abstract: The molecular geometries (bond distances and bond angles) of N^{α}-acetyl-*N*-methylalaninamide were refined in seven characteristic areas of its conformational space by ab initio gradient relaxation at the 4-21G level. The optimized conformations in order of increasing energy are C_7^{eq} (I), C_5 (II), C_7^{ax} (III), β_2 (IV), α_R (V), α_L (VI), and α' (VII). The variations in local geometry found between the conformations investigated are discussed in detail. It is found that comparable bond distances and bond angles in different conformations can vary by 0.025 Å and up to 7.5°, respectively. Small deviations from planarity of the peptide group (up to 8°) are found for some of the conformations. The calculations confirm a previously suggested correlation between the ϕ and ψ angles in the helical forms of the dipeptide, which is in agreement with observed protein structure data and high-resolution crystal structures of small polypeptides. Details in the refined local geometries confirm that it is reasonable to rationalize this correlation in terms of a dipeptide specific intramolecular interaction between atoms N7 and H18 (Figure 1). This interaction, which is directed perpendicularly to the peptide bond, may be an important contribution to the formation and stability of bend type structures in proteins. The significance of the variations in local geometry for empirical conformational analysis of proteins is discussed.

In the last decade it has become common practice to investigate the conformational and structural features of peptides by computational methods. Model dipeptides and other systems have been studied by limited basis set ab initio methods,[1-4] as well as by many different semiempirical and empirical methods.[5-8] These calculations have given us a general understanding of conformational parameters at low-energy minima in the conformational space. However, little detailed information is available for comparing the effects of changes in conformation on the local geometry of the peptide. This is true even when considering high-resolution experimental data found from crystal structures, where a variety of conformations for equivalent molecules are simply not found.

For molecules larger than dipeptides, one must move away from rigorous computational studies into the area of empirical energy calculations, where approximations of forces and geometries are only as good as the data and equations used to define the force field. Empirical methods are necessary if one wishes to study larger molecular systems simply because the rigorous methods are incapable of handling a large number of atoms at a reasonable computational expense. Thus, empirical methods have been used to find low-energy conformations of polypeptides containing up to ~14 amino acids[9,10] and have been used in protein structure refinement studies.[11]

The study described here on the molecule N^{α}-acetyl-*N*-methylalaninamide (Ala) is an attempt to fill in some important gaps in our understanding of peptide structure. One point of interest, for example, concerns the variations in local geometry

[†] University of Arkansas.
[‡] Memphis State University.

(1) Schäfer, L.; Van Alsenoy, C.; Scarsdale, J. N. *J. Chem. Phys.* **1982**, *76*, 1439-1444.
(2) Peters, D.; Peters, J. *J. Mol. Struct.* **1979**, *53*, 103-119; **1980**, *69*, 249-263; **1980**, *62*, 229-247.
(3) Peters, D.; Peters, J. *J. Mol. Struct.* **1981**, *85*, 107-123.
(4) Shipman, L. L.; Christofferson, R. E. *Theor. Chim. Acta* **1973**, *31*, 75-82.
(5) Pullman, B.; Pullman, A. *Adv. Protein Chem.* **1974**, *28*, 347-526.
(6) Yan, J. F.; Momany, F. A.; Hoffman, R.; Scheraga, H. A. *J. Phys. Chem.* **1970**, *74*, 420-433.
(7) Scheraga, H. A. "Peptides"; Goodman, M., Meinenhofer, J., Eds.; Wiley: New York, 1977; pp 246-256.
(8) Momany, F. A. *Top. Curr. Phys.* **1981**, *26*, 41-79.
(9) Momany, F. A. *J. Am. Chem. Soc.* **1976**, *98*, 2990-2996.
(10) Momany, F. A.; Drake, L. G.; AuBuchon, J. R. *Int. J. Quantum Chem., Quantum Biol. Symp.* **1978**, *5*, 381-391.
(11) Warme, P. K.; Momany, F. A.; Rumball, S. V.; Tuttle, R. W.; Scheraga, H. A. *Biochemistry* **1974**, *13*, 768-782.

0002-7863/83/1505-3438$01.50/0